

Efficient electrostatic-mechanical modeling of C-V curves of RF-MEMS switches

Jeroen Bielen, Jiri Stulemeijer

NXP Semiconductors

Gerstweg 2, 6534 AE Nijmegen, The Netherlands

Tel: +31 24 353 6626, Fax: +31 24 353 6556, E-mail: jeroen.bielen@nxp.com

Abstract

The capacitance versus actuation voltage, the C-V curve, is characteristic for the steady state behavior of a RF-MEMS capacitive switch. It is imperative to have an efficient method to simulate these curves and overcome the convergence problems from pull-in and release instability that is inherent to these electrostatic actuated devices. In this paper we show how the complete CV curve can be calculated in FE code, including conditionally stable parts and zipping regions, which also comprises a non-linear contact model. Efficiency improvement by use of a reduced order model for the electrostatic domain is shown. Validity of the simulation results is shown by comparison to measurements.

1. Introduction

For future ambient intelligent RF-applications, the use of capacitive RF-MEMS switches (Figure 1) is gaining increased attention since these pose a means to e.g. create adaptive antenna matching and reconfigurable RF circuits [1]. Part of this attention is due to the large on-off capacitance ratio that can be realized with this class of MEMS ($>1:20$), which means the device is in full contact with the bottom dielectric in the activated state. From a modeling point of view means that the open behavior of such a switch must be described accurately, but also the (partially) closed state and the transitions between these states that determine important properties such as release voltage. The release part is not only of interest because of the voltage, but also to identify potential partial release states where sticking can occur when the dielectric gets charged (an undesirable phenomena). This is closely related to the presence of the conditionally stable parts.

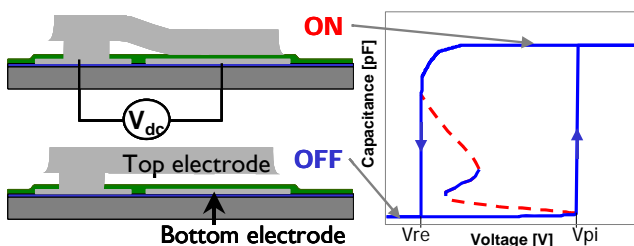


Figure 1: Schematic drawing of electrostatic switch and CV curve with conditionally stable parts in dashed red.

At the pull-in voltage a fold in the C-V curve exists. Trying to find the exact pull-in voltage by applying a voltage sweep and using adaptive stepping until there is no longer convergence requires a large computational effort and is inefficient. A number of methods to overcome this have been reported in literature. Notably, Elata et al. ([2],[3]) introduced the displacement iteration

scheme (DIPIE). The underlying idea of this method is that instead of prescribing a voltage, a displacement constraint is prescribed and a voltage is solved for (Figure 3). This algorithm can be implemented in FE codes by scripting.

This paper presents a DIPIE+ algorithm capable of simulating the entire CV curve of a large variety of devices including stable or conditionally stable parts of the release trajectory. Additional to the DIPIE algorithm a second adaptive algorithm for selecting the location of the control node is introduced in order to allow the iteration scheme to continue after initial contact.

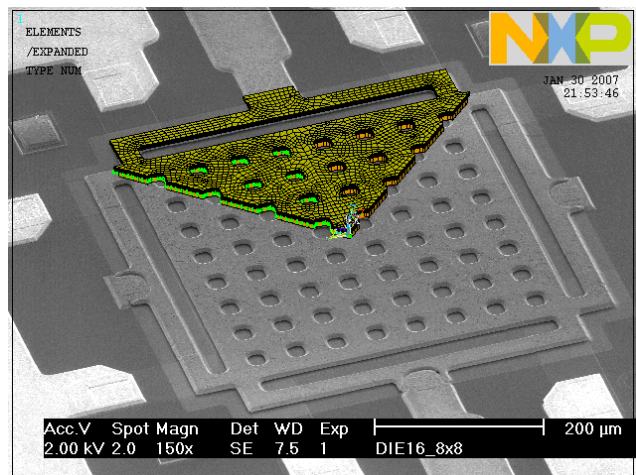


Figure 2: RF-MEMS capacitive switch. FE model overlaid on SEM image of an 8x8 device

Further efficiency can be gained in the implementation of the electrostatic mechanical coupling. Despite the deformation of plate and beams the structure remains to good approximation parallel to the substrate. Based on this observation a reduced order model can be derived. With a detailed electrostatic model that is solved for a small number of gaps, the charge as function of gap is derived for every node in the coarser meshed mechanical model. This reduced order model is subsequently used in the much smaller directly coupled electro-mechanical model for which the DIPIE+ scheme is used. Simulating the entire CV curve requires up to several hundreds of iterations, that are performed on a significantly reduced model. This results in an efficient way to include fringe fields.

A large range of topologies of devices can be solved with this scheme. The simulated results obtained with Ansys have been verified with measurements on various devices. The presence of stable parts in the C-V curve can depend on initial deformations and temperature as will be shown.

2. Method

As shown in the paragraph before, electrostatic switches have an inherent hysteresis, causing the pull-in and release voltage to be different. The states in between the open and close state are unstable. For a 1-D problem, a rigid plate suspended by a spring, the steady state equilibrium between mechanical forces F_m and electrostatic force F_{es} is given by:

$$F_m + F_{es} = k \cdot (z - \text{gap}0) + \frac{\epsilon_0 \cdot \text{Area} \cdot V^2}{2 \cdot z^2} = 0 \quad (1)$$

Equation 1 has no unique solution of displacement z when voltage V is prescribed, but it has an unique solution for $V(z)$, as depicted in Figure 3.

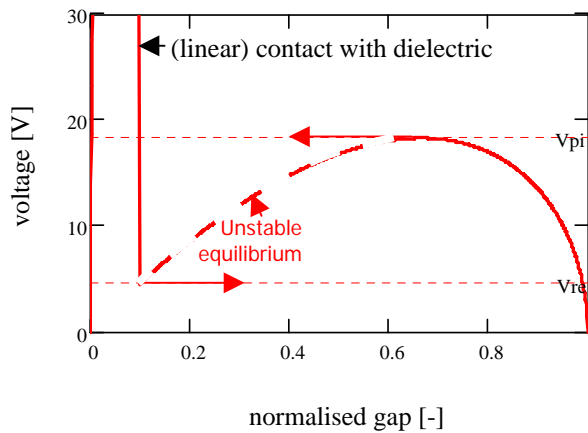


Figure 3: The idea behind the DIPIE algorithm: A prescribed displacement only allows for one equilibrium voltage where a prescribed voltage may have multiple displacements as solution.

One method to calculate the pull-in voltage of an arbitrary shaped electrostatic switch is by applying a voltage sweep, and running the simulator until no convergence is reached. A much more efficient method is introduced by Elata et al [2,3] and termed DIPIE algorithm. Although Figure 3 will not hold for any node in a full 3D structure, the principle of prescribing displacement on one node and searching the voltage that minimizes the reactive force can still be applied in 3D problems, provided a proper control node is used (Figure 5). This graph shows how by first using node 1 to prescribe displacement until it reaches contact and then switching to 2, all equilibrium states can be found.

The DIPIE algorithm is easily implemented in any FE code that has some scripting capability. A displacement is prescribed for the control node and a guess value for the voltage is applied. With a prescribed displacement and in the absence of pull-in instabilities, the FE solver will quickly converge to a solution from which the reaction force on the control node can be retrieved. A simple Newton iteration method then is used to calculate the next voltage estimate to feed to the FE solver. This is repeated until the reaction force is below some error norm.

For an actual 3D FE model however, it is not always guaranteed that the optimal node is (or can) be selected to

prescribe the displacement. This may result in pull-in and release hysteresis of a different part of the structure without a nodal displacement prescribed while the Newton scheme attempts to search the voltage that nullifies the reaction force. This means there are potentially two voltages that will have a zero reaction force, the correct solution being the one closest to a previous state. In order to find the correct voltage, a step back in the Newton algorithm needs to be enforced. Since the FE model switches from the 'good' (based on shape or capacitance) to the 'wrong' state when such pull-in is encountered, it needs to be set back to the previous solution of the 'correct' state. This is implemented by using a single frame restart whenever necessary and switching to a regula falsi search algorithm. This approach works quite well, on the expense of convergence speed however.

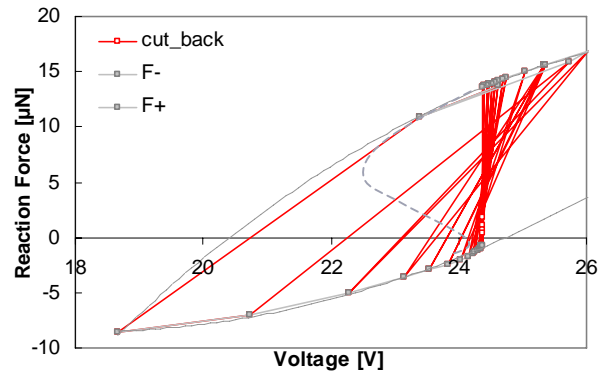


Figure 4: Reaction force versus voltage during Newton iterations with cut-back initiations; the x-axis intersection at 24V is the searched zero and can only be found if the simulator is 'reset' to the lower trace.

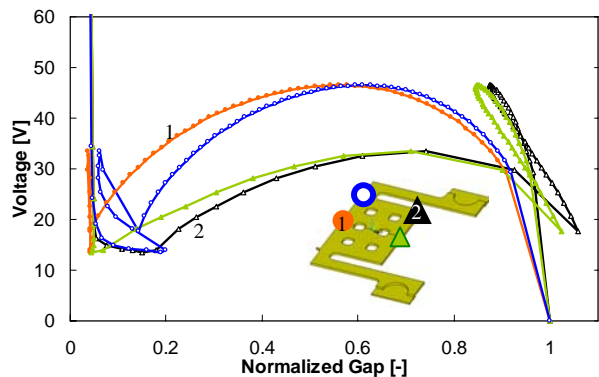


Figure 5: Equilibrium voltage versus gap for four nodes on a device with mode shape changes: Unique voltages can only be found if an appropriate node is used to prescribe displacement.

Control node selection

However, this DIPIE algorithm as described only allows the extraction of pull-in voltage, and not possible additional stable parts of the CV curve at the release part or during zipping. Examples of devices that exhibit such behavior are single cantilevers that can possess a stable state after an initial pull-in when the tip touches the substrate and have a second pull-in resulting in part of the

beam in contact with substrate. The beam can zip into further contact with increasing voltage. In order to find these other stable solutions, the entire CV curve, including conditionally stable solutions needs to be calculated.

The DIPIE algorithm as described above is useful for finding the pull-voltage, but cannot find any solutions of the release once the control node has contacted the bottom. Using a node at the side of the plate is not an adequate solution since this will fail to stabilize the centre of a flexible plate. In order to find those solutions, all nodes of the plate must ultimately reach contact so the control node must be adaptively selected.

Three different criteria for selecting the best control node were compared. The most obvious is to take the lowest point of the plate, since this experiences the largest electrostatic pressure. Alternatively, the selection can be based on previous converged displacement iterations. This leads to considering either displacement increment or increment of electrostatic force, the latter possibly being a measure for how quick a location approaches pull-in. Although there were differences in the convergence speed, none of the selection criteria good prevent (i.e. predict) a pull-in hysteresis to occur during the successive displacement iteration, while the voltage was changed to minimize the reaction force. With the topologies that we evaluated, the electrostatic force increment appeared the best criteria.

3. Experimental

Measurements of steady state CV curves presented here have been done on a wafer prober at low frequency under controlled ambient. In the used set-up an LCR meter is used at typically 1MHz to measure the capacitance. A bias voltage is applied externally and slowly stepped with steps of 0.5V or 1V to well above the positive and well below the negative pull-in. Parasitic capacities are characterized by removing the plate of a device and measuring the capacitance again, although de-embedding of S-parameters measured at 1GHz is also used.

During the CV measurements, the dielectric of the device may experience charging, an undesirable phenomenon that is often prevented by applying bipolar actuation [7]. In the CV measurements this will result in both a shift but also ‘narrowing’ of the voltage axis when one device is measured several times. When characterizing the temperature dependency, CV curves should be corrected for this effect. In the presented measurements this is done by calculating the charging related voltage shift from CV measurements at room temperature before and after the measurement.

4. FE model

The previously described DIPIE+ algorithm has been implemented in Ansys90 by using APDL (Ansys Parametric Design Language). The FE model consists of two FE models that both use the same solid model geometry. One model of the electrostatic domain is used to calculate the capacitance versus gap when the plate

receives a uniform vertical displacement. The second model is an (directly coupled) electro-mechanical model that uses the results of the other model for the transducer characteristics. This latter model uses the DIPIE+ algorithm to calculate the CV curve.

Geometry of the models is either fully parametric or imported from CAD drawing. Both physics domains take advantage of any symmetry that applies, either rotational (with help of constraint equations) or 1/8th normal symmetry. Local coordinate systems are rotated accordingly and are taken into account for the DIPIE displacement DOF.

Electrostatic model.

When assuming that the plate is to good approximation parallel to the bottom electrode, the electrostatic domain can be effectively captured in a reduced order model that describes the capacitance versus gap of each node on the mechanical model. For this purpose an electrostatic model was build, and looped with a gap ranging from just the effective air gap on closure up to completely open.

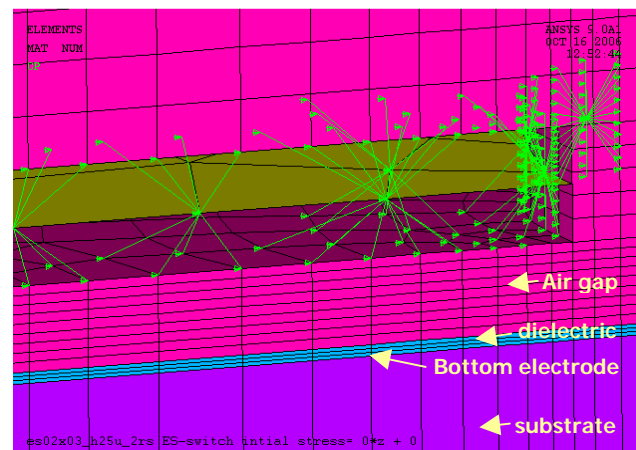


Figure 6: Electrostatic model. Arrows indicate how charge is assigned from the electrostatic nodes to the nearest ‘mechanical’ node (shell elements at the plate mid-surface).

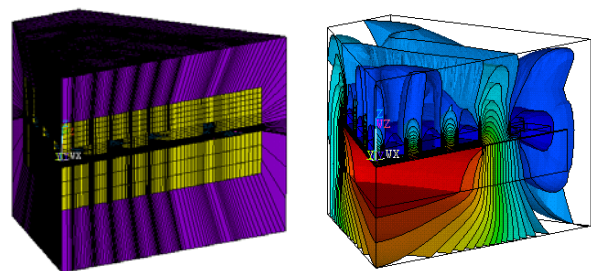


Figure 7: Electrostatic model and iso-potential surfaces

This electrostatic model needs a finer mesh near the edge of the holes than the mechanical model and hence has a different mesh. The charge in each node of the electrostatic calculation is mapped to the closest node on the bottom of the plate of the mechanical mesh. This guarantees that the total capacitance is correct and charge is conserved (this mapping process is schematically

depicted in Figure 6). Since there always remains some effective air gap due to microscopic roughness, the electrostatic model does not need to be solved for a completely closed gap. Therefore morphing one and the same mesh can simulate the entire range of the gap.

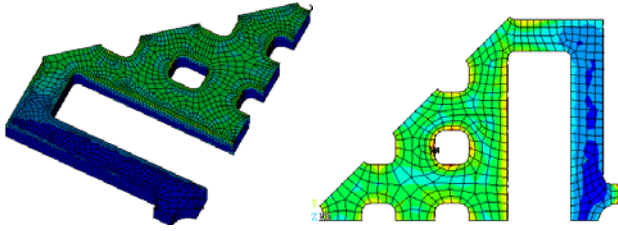


Figure 8 Charge distribution @ IV (=capacitance) of the ES model (left) and charge density as transferred to the mechanical mesh (right)

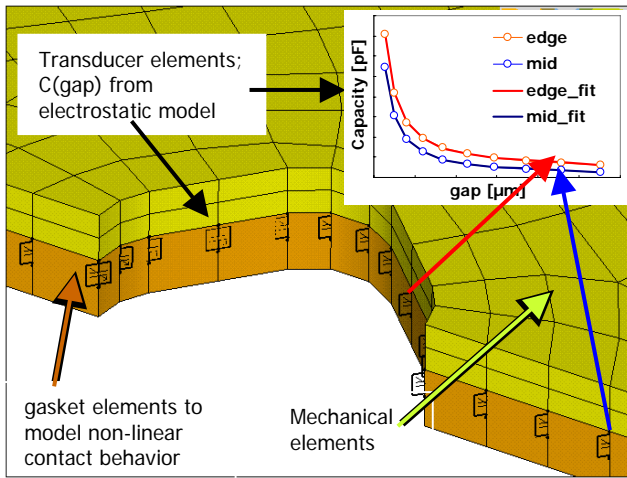


Figure 9: Detail of electromechanical model and an example of the $cap(gap)$ relation used for the transducer elements (inset).

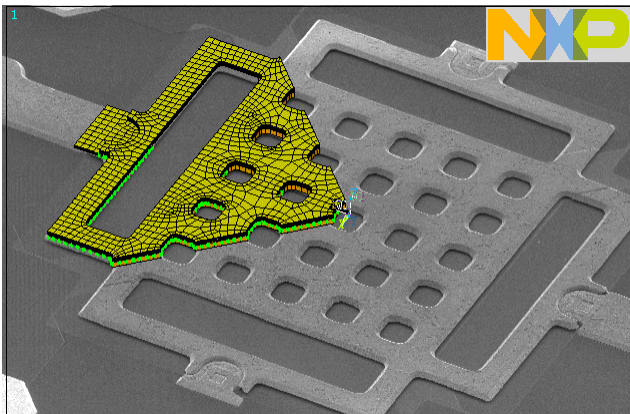


Figure 10: FE model overlaid on SEM image of the 5x5 device

Far field effects are modeled with so called infinite elements that account for the correct boundary conditions of exterior faces of the model. The plate receives zero voltage in order not to add far field capacitance contributions to the plates charge. The only relevant material property in this model is the relative dielectric

permittivity of the dielectric which was measured on some MIM caps.

Electro-mechanical model

The mechanical model is depicted in Figure 9 and pretty straightforward. As long as the primary interest in this simulation is not the stress levels, but the CV curve, the element divisions in the thickness direction of the plate is not very relevant. Element division in x and y do affect the CV curve. Material properties have been measured on special single cantilever structures using a nano-indenter (reported in [4]).

The transducer elements receive their $C(gap)$ from the electrostatic simulation (passed through a table). The table is approximated by Ansys with a function: $Cap(gap)=c_0/gap+c_1+c_2 \cdot gap+c_3 \cdot gap^2+c_4 \cdot gap^3$ (2) This provides an adequate fit for adding fringe field effects to a parallel plate equation. The gap of the mechanical model also includes the dielectric i.e. $gap=gap_air+gap_diel/eps_diel$. Since the number of transducer elements is much smaller than the number of elements in the electrostatic model, this approach saves over 100k DOF;s for the model on which the DIPIE algorithm is run.

Non-linear contact model

An important feature of the actually measured CV curves that we also wanted to capture in the model is the dependency of C_{close} on voltage. This is caused by bending of the plate around small features that protrude from either of the surfaces and from the non-linear contact deformation. As the effect is equally present in small devices, this deformation behavior of the microscopic roughness is thought to be dominant.

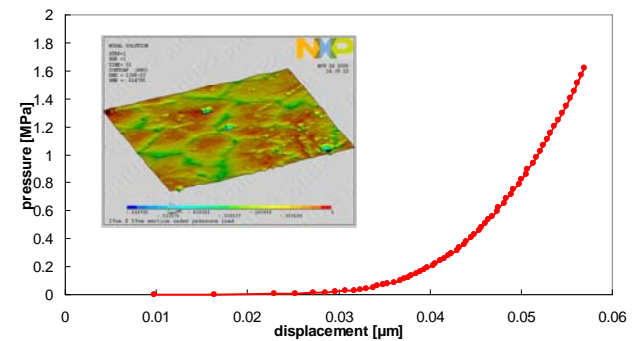


Figure 11: Measured contact pressure versus (electrostatic) gap is caused by microscopic roughness (inset is AFM profile) and can be approximated with an exponential relation.

Therefore, in analogy to [6], a non-linear spring needed to be introduced as contact element since this effect cannot be captured when contact is modeled with linear contact penalty stiffness i.e. the default contact in the transducer element is inadequate. In Ansys a multi-linear gasket element is suited for this purpose although a 1D non-linear spring can be used as well. Properties were extracted from the close part of a CV curve (Figure 11) using equation 1 and parallel plate approximation for C.

5. Results

Electrostatic results

A typical result of the electrostatic model, capacitance versus gap, is shown in the inset of Figure 9. The values of the capacitance calculated with Ansys is within 1% of values calculated with more dedicated software for HF simulations i.e. Sonnet.

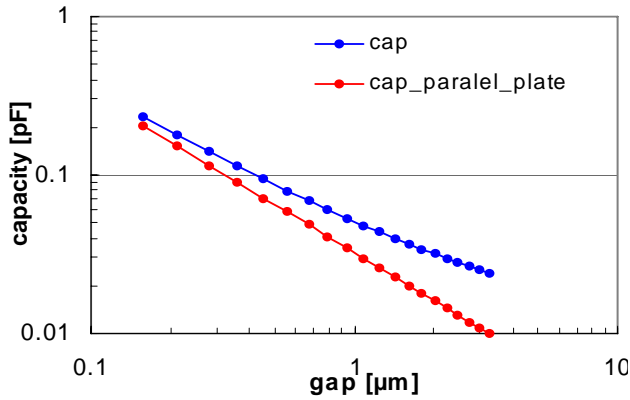


Figure 12: Simulated capacitance versus gap of 2x2 device showing significant contribution of fringe fields to total capacitance

Mesh size sensitivity evaluation was done for both the electrostatic and mechanical model which resulted in the used mesh. It turned out that for the mechanical mesh, if only the CV curve is of interest, and in absence of stress gradients, the plate can be modeled with solid shell elements (1 division in thickness). Lateral element division must suffice to capture roll-off effects caused by the holes i.e. at least 2 elements per side of the holes. Absorbing the holes in an effective Young's modulus is therefore less accurate.

Measured & simulated CV curves

For validation of the model, simulations were compared to measurements of four different device layouts, ranging in size from 2x2 up to 8x8. From CV measurements on several wafers, a typical device was selected for each layout. In order to have an accurate model the exact realized geometry of these devices was measured in a SEM.

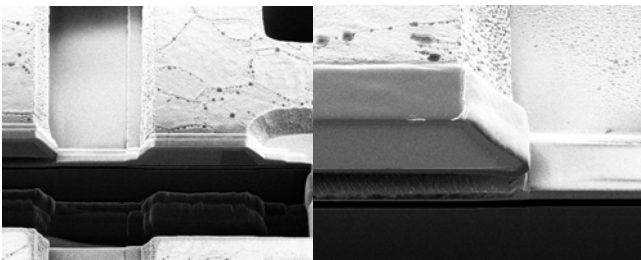


Figure 13: Image of FIB cross-section of a beam (in pull-in due to charging by the FIB) showing the inclined sidewalls.

Layer thickness was measured on FIB cross-sections. The sidewalls of the metal are inclined (Figure 13) but the model has straight walls. To account for this effect, the effective width in terms of second moment of inertia was taken for the beams (=mechanical cross-section). For the

plate, the bottom width was taken since here the electrostatic forces are quantitatively most important.

In addition to these SEM/FIB measurements, the initial bow of the plate was measured with a white light interferometer. These deformations were included in the model by introducing an (uniform) initial stress gradient. In principle it is possible to predict this initial shape as well with FE simulations of the processing steps, but this is considered a different topic and beyond the scope of this paper. The initial deformation of the beams was included in the initial gap by offsetting the entire structure. This approach can be justified by considering that the beams do not undergo large rotations or experience other non-linear effects.

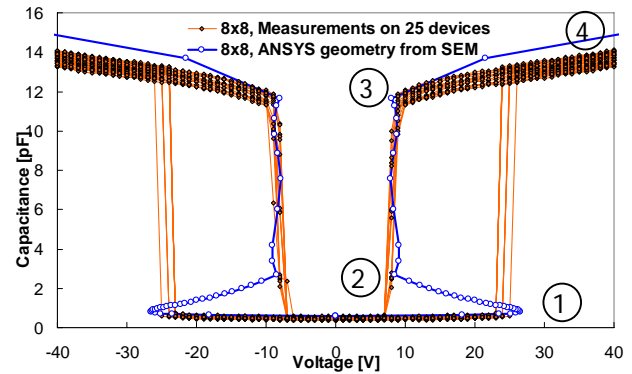


Figure 14: Measured and simulated C-V curves of an 8x8 reference device

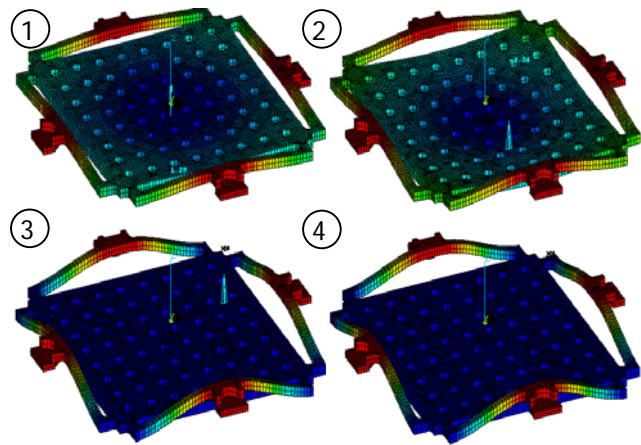


Figure 15: Z-displacement of 8x8 device at four stages depicted in the CV curve of Figure 14

The measured and simulated C-V curves of a 5x5 and an 8x8 device are depicted in Figure 14 and Figure 16. It can be seen that there is good agreement between simulations and measurements. Difference in the close capacitance can be caused by difference in micro roughness of just 10nm (for all simulations the same contact model was used). The pull-in and release voltages can be altered significantly by changing the geometry marginally, possibly less than the accuracy of the geometry measurements. Furthermore, when CV curves show a lot of steps in the release trajectory, the measured

release voltage is strongly dependent on the definition and algorithm used to extract it from the measured CV curve.

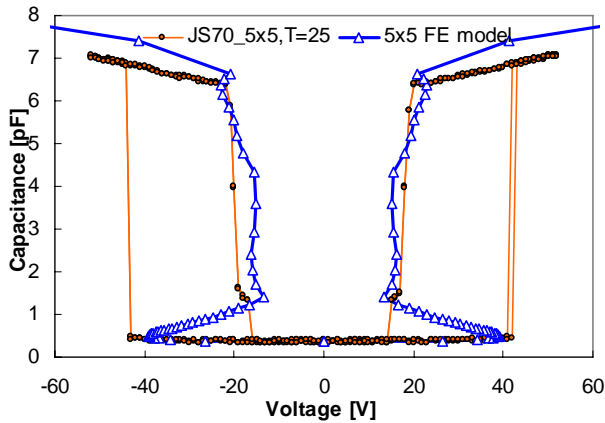


Figure 16: Measured and simulated C-V curves of a 5x5 device

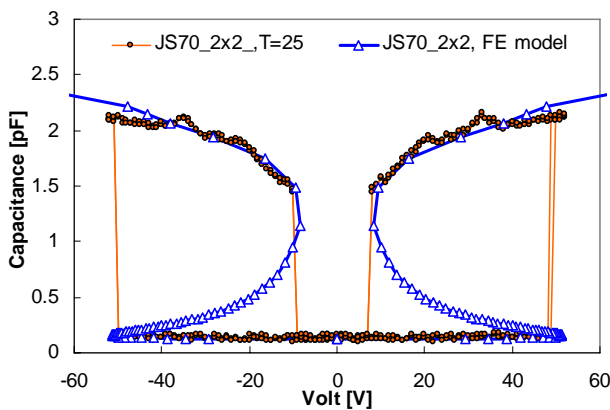


Figure 17: Measured and simulated C-V curves of a 2x2 device

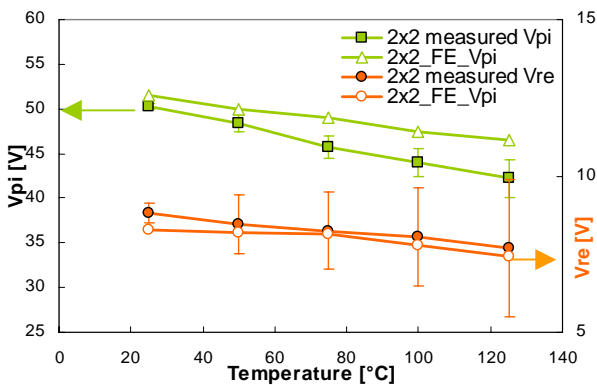


Figure 18: Measured and simulated temperature dependencies of pull-in and release voltage of 2x2 device.

6. Outlook

The presented DIPIE+ algorithm has been applied on various topologies. Although a proper control node selection is essential for finding the equilibrium state, it cannot solve any problem. For example systems that tend to have strong changes in the bending modes or have buckling behavior, like plates tilting around a hinge, still

pose problems regardless the control node selection criteria. In those cases several nodes, that are only weakly coupled by the structure itself, may require a prescribed displacement to stabilize it while searching for the voltage to nullify the reactive force on another node. We are currently working on a nesting method of the presented algorithm to stabilize multiple nodes.

7. Conclusions

A displacement iteration scheme with adaptive control node selection that is able to calculate the entire CV curve of real-live topology electro-static switches has been presented. We showed that, with the inclusion of a non-linear contact model, an accurate match with measurements is reached, also in the partial or full contact regimes of the curves. The inclusion of fringe field effects can be achieved by deriving a reduced order model from an electrostatic model that is morphed. Temperature or packaging effects can be taken into account in the mechanical model. This provides a powerful, computationally efficient tool to predict functional parameters of various device types and moreover can certify the design performs well against specifications.

Acknowledgement

Special thanks go to the NXP IC-RF MEMS team, specifically to Ramon Havens for performing the measurements.

References

1. J.T.M. van Beek, P.G. Steeneken, G.J.A.M. Verheijden, J.W. Weekamp, A. den Dekker, M.Giesen, A.J.M. de Graauw, J.J. Koning, F.Theunis, P. van der Wel, B. van Velzen, P. Wessels, "MEMS for wireless communication: application, technology opportunities and issues", *European Microwave week 2006*, Manchester.
2. Elata, D., "Modeling the electromechanical response of RF MEMS", *Eurosime2006*, Como, Italy, 2006.
3. Elata, D., Leus, V., "Switching time, impact velocity and release response of voltage and charge driven electrostatic switches", *IEEE ICMENS'05*.
4. Burg, V., den Toonder, M., van Dijken, A., Hoefnagels, J., Geers, M., "Characterization of free-standing thin film material properties for RF-MEMS", *Eurosime2006*, Como.
5. AnsysTM90 theory manual, Ansys Inc.
6. Chan, E.K., Garikipati, K., Dutton, R.W., "Characterization of Contact Electromechanics Through Capacitance-Voltage Measurement and simulations", *J.of MEMS*, Vol.8, No.2, June1999.
7. DelRio, F.W.; Herrmann, C.F.; Hoivik, N.; George, S.M.; Bright, V.M.; Ebel, J.L.; Strawser, R.E.; Cortez, R.; Leedy, K.D, "Atomic layer deposition of Al/sub 2/O/sub 3//ZnO nano-scale films for gold RF MEMS", *IEEE MTT-S International*, Vol.3, June 2004.
8. Greenwood, J.A., Williamson, J.B.P., "Contact of nominally flat surfaces", *Proc.R.Soc.A*, Vol295, 1966